1 Introduction

Light microscopy is an important tool in biology and medicine. Because light interacts with cells and tissues without damaging them, investigation of a biological system while it is alive is made possible through light microscopy. However, the physics of the lens imposes important limitations on conventional light microscopy. This thesis presents a novel light microscopy technique aimed at overcoming these limitations and enabling previously impossible investigations.

2 Background

Four key performance parameters of microscope lenses are resolution, depth of focus, working distance, and field of view. These are intrinsically entangled and controlled by the *cone angle* of light collected by the lens (figure 1). As a result, high resolution, which is desirable, requires short working distance and small field of view, both of which are undesirable, if the size of the lens remains the same.

During the last decade, a great deal of effort has been expended to enhance the resolution of light microscopes. Image restoration (deconvolution) has became an established technique for undoing the effect of three-dimensional point spread function [**1, 8, 2**]. Engineering the point spread function itself has also been successfully demonstrated. Examples are confocal microscopy [**15**] and novel variations of it such as two-photon microscopy [**4, 3**] and 4Pi microscopy [**7**]. Recently, Frohn [**6**] demonstrated the use of a mesh-like interference pattern as an illumination pattern for enhancing the resolution of fluorescent microscopy. However, all of the above efforts continue to rely on precision optics as the primary source of resolution.

There have been several attempts to produce high resolution images without precision optics, using so-called 'lens-less imaging' approaches. Borrowing the concept of synthetic aperture radar, Turpin proposed the synthetic aperture microscopy (SAM) [**14, 13**]. In this method, the sample is illuminated by a laser beam and an image is generated by analyzing how the coherent light rays reflected from target features in-

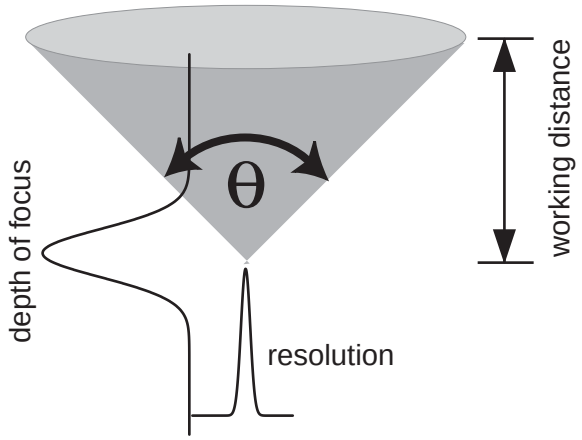

Figure 1: The cone angle (angle θ) controls resolution, depth of focus, working distance, and field of view. Resolution refers to the minimum separation distance of two infinitesimally small objects. Depth of focus is the range of axial (*along the optical axis*) distances over which the sample stays in focus. Two curves represent intensity profiles of the three-dimensional point spread function (PSF) along lateral and axial directions. The narrower the width of the curve, the higher the resolution and the smaller the depth of focus. Working distance is the distance from the sample to the instrument. Field of view is the area of the sample that can be viewed in a single picture. The cone angle defines the solid angle over which light gets collected through the lens.

terfere with each other. However, computational complexity is still a major problem [**14, 10**], and no image generated based on this method has been reported yet. Another method, proposed by Hutchin [**9**], illuminates the sample with two interfering laser beams, rather than a single beam, and a low resolution detector is used to record the sample's response modulated by the fringe pattern. In principle, resolution of the reconstructed image is determined by the bandwidth of the illumination, not by the aperture of the lens (figure 2). Even though computationally less complex than the one beam case, implementation of the concept is still a difficult problem. To the best of my knowledge, there are no reports of images generated using this concept. The main challenges are

1. Generation and projection of sufficiently large number of optical patterns.
2. Fast enough switching between patterns in the set.
3. Nano-meter precision in knowledge of projected pattern.

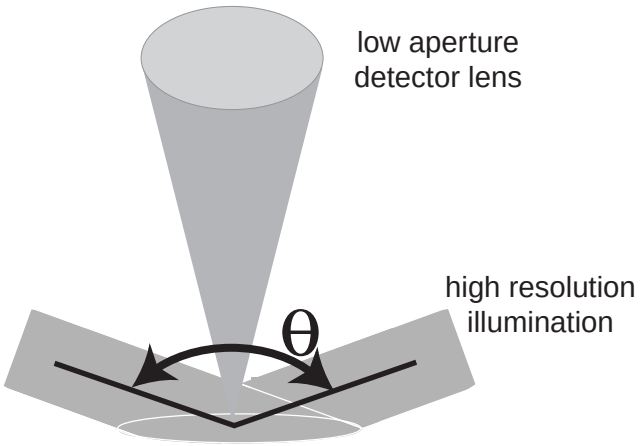

Figure 2: High resolution images using low aperture lens. A high resolution laser interference pattern is used to illuminate the sample, while a low aperture lens is used on the detector side. Resolution of the image is determined by the highest spatial frequency of the illumination pattern which is controlled by wavelength of the light and the angle θ.

Our laboratory has developed a promising way of generating and controlling multiple beams for projecting high resolution interference patterns produced by several

dozen beams [**11**]. The beam delivery architecture of a prototype projector is shown in figure 3. In this setup, an acousto-optic modulator (AOM) is used to split a single beam into multiple diffracted beams, whose amplitudes and phases are controlled by electrical signals that drive the AOM. An assembly of mirrors is used to convert an array of beams into a converging cone of beams, creating an interference pattern at the sample region. Preliminary data from this setup can be found in [**11, 12**]. The scope of this project includes both engineering the projector and using it to generate images. The term synthetic aperture microscopy (SAM) will be used throughout this document to refer to the resulting novel light microscopy technique.

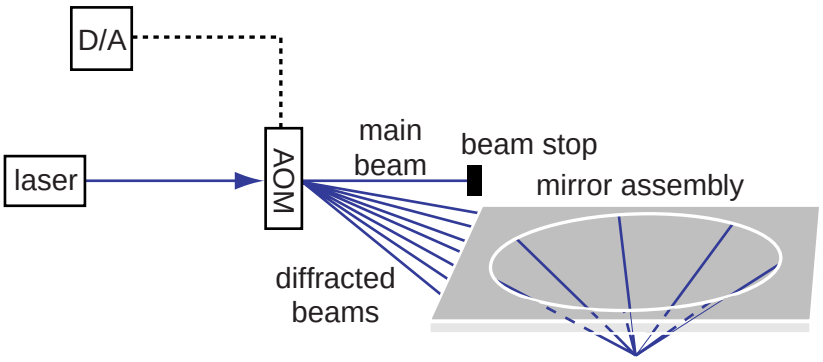

Figure 3: Acousto-optic interference pattern projector [**11**]. Acousto-optic modulator (AOM) generate an array of diffracted beams from a single laser beam. An assembly of mirrors converts an array of beams into cone of beams to project interference pattern (D/A: radio frequency waveform generator).

3 Proposed work

The overall goals of this thesis project are the generation of high resolution images without precision optics and the application of the method to a biomedical imaging problem. Three phases of the project in achieving these goals are listed as the following specific aims:

1. Calibration of high resolution pattern using low resolution optics.

2. Generation of images and demonstration of super-resolution.

3. Application to biomedical imaging.

3.1 Calibration of high resolution patterns of light using low resolution optics

Our prototype projector in figure 3 allows us to project a rich set of high resolution interference patterns using several dozen laser beams. However, we cannot make use of patterns without knowing exactly what they are. Building a mechanical system that controls amplitudes, phases and directions of beams with nano-meter precision is not practically possible. Even if this could be done, small environmental perturbations such as temperature fluctuations will make the system change over time. Therefore, a calibration method needs to be developed to overcome mechanical imperfections by actually measuring the beam parameters in the area where they overlap. Furthermore, the following requirements need to be met: 1) Calibration should not rely on high precision optics. 2) Calibration should be sufficiently fast, so that it can be done routinely.

I have developed a calibration method that uses only a sparse array of fluorescent microbeads without adding any further complexity to the setup (figure 4). In this setup, a low resolution lens is used, which cannot resolve either the projected pattern or the beads. The size of the bead is comparable to the wavelength of the light, so that the bead can spatially sample the pattern. The role of the lens and the camera is simply to count the number of photons coming off the bead, which is recorded as the brightness of the pixel that contains the bead. This provides raw data which can be further analyzed to estimate the amplitude, phase, and direction of each beam. An iterative search algorithm was developed to estimate the directions of the beams, as well as the sub-pixel locations of the beads, starting from crude initial guesses. The method was then used to dynamically assess mechanical imperfections of the physical setup.

Expected challenges. The current combination of the AOM and the beam delivery setup can produce up to 35 beams. However, previous measurements indicate that these beams differ in cross sectional shape, amplitude, and path length. As a result many beam combinations fail to produce usable interference patterns. An etalon was installed to increase the coherence length of the laser. Experiments will determine whether this solves the problem. I plan to use a set of neutral density filters ('light attenuator') and adjust the AOM drive signal to maximally equalize beam amplitudes. Figure 5 shows the beam geometry and the resulting sample points in Fourier space for the proposed 35 beam SAM.

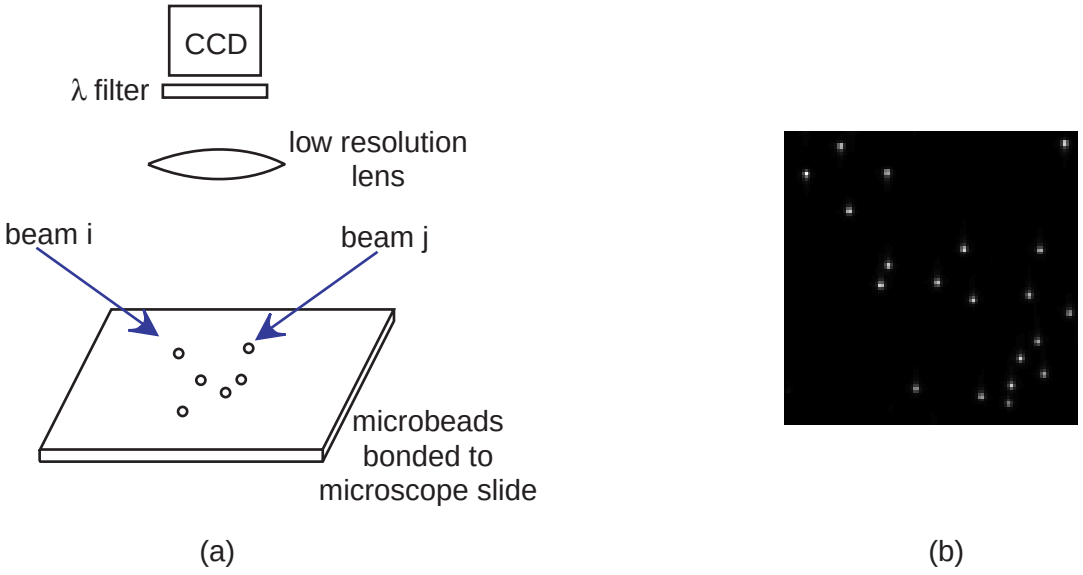

Figure 4: Microbead calibration method. (a) Setup. Fluorescent microbeads (Molecular Probes, Eugene, OR) are bonded onto a microscope slide. A low resolution lens and CCD camera record the brightness of the beads when illuminated by the interference pattern. Two laser beams are shown. A color glass filter (CVI laser, Albuguergue, NM) is used to remove light other than the fluorescence of the bead. (b) CCD image of the bead sample when illuminated by a two beam interference pattern showing 20 isolated beads. The shapes of the beads are not resolved and the location of the beads are not known with sub-pixel accuracy.

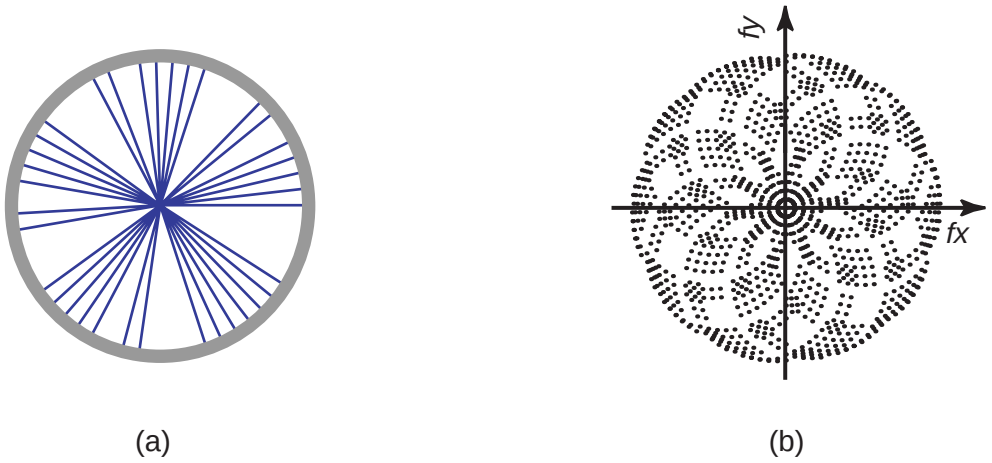

Figure 5: Beam geometry seen from the top (a) and resulting Fourier samples (b) for 35 beam SAM. In panel (a), each line represents a laser beam. 35 beams are shown to overlap at the center of the ring. In panel (b), each dot represents a sample point in Fourier space. A pair of beams produces three points in Fourier space, two mutually conjugate points and a point at DC. For 35 beams, there are ${}_{35}C_2$ points in panel (b).

3.2 Generation of images and demonstration of super-resolution

In the second phase of the project, high resolution images using low aperture lens will be demonstrated by comparing images acquired with 1) *low* resolution lens and *diffuse* illumination 2) *low* resolution lens and *structured* illumination 3) *high* resolution lens and *diffuse* illumination.

A sample made of fluorescent microbeads will be used as the test target. These beads are readily available in various sizes with different spectral characteristics. Controlling the sizes and concentration during the preparation step allows us to fabricate various samples that simulate imaging of biological samples.

As seen in figure 5, the distribution of sample points in Fourier space is highly non-uniform. Complete understanding of the effect of nonuniform sampling on image reconstruction and how to deal with it is not available yet. So far, two approaches have been worked out to address this issue. First, one seeks to find a geometrical arrangement of beams that results in sampling characteristic in Fourier space that is as uniform as possible. An example is shown in figure 6. The second approach

accounts for the sampling density non-uniformity in image reconstruction. Computer simulations have shown that weighting Fourier coefficients based on sampling density improves reconstructed image as shown in figure 7. I plan to use the current geometry of beams as shown in figure 5 and the weighting method in image reconstruction for generating images. Further refinement of either the geometry of beams or the image reconstruction algorithm will be pursued, if necessary, and if time allows, after the first generation of images are acquired.

Expected challenges. The issue of how to select a minimal set of patterns with which to interrogate the sample and how to interpret measurements to determine the Fourier coefficient needs to be worked out. Thorough understanding of this topic is a prerequisite for reconstructing images and important for practical reasons such as the speed of data acquisition.

3.3 Application to biomedical imaging

An effort to achieve high resolution without sacrificing other parameters of microscopic imaging is very timely given recent changes in biomedical sciences. Through the past several decades, key biological actors at molecular scale have been identified and their functions have been extensively studied. However, it is becoming increasingly important to understand how these actors interact with each other at a large scale. Conventional optical microscopy cannot address this demand adequately and SAM holds promise in this regard, with some additional important advantages.

So far, I have identified two possible biomedical imaging applications which the current SAM is suited for. These are DNA microarray and *in vitro* culture of neurons (figure 8). These samples are planar in structure, the imaging targets are fluorescently labeled, and importantly, require high resolution investigation over a large area. I will be focusing on exploiting SAM's capability in acquiring biologically meaningful information that is not possible to obtain using conventional microscopy. For example, SAM could turn out to be a highly sensitive way of detecting fluorescence without causing photodamage and photobleaching, an important issue in fluorescent

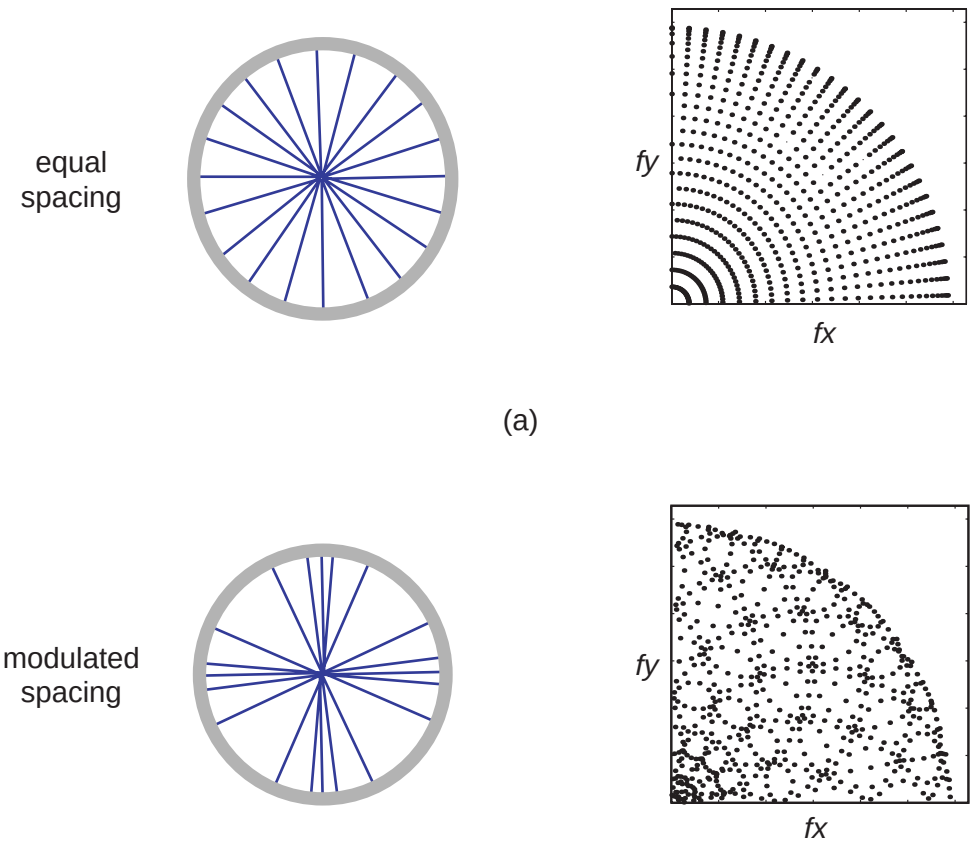

Figure 6: Effect of beam geometry on sampling density. (a) Equally spaced beams and resulting sample points in Fourier space. Only the first quadrant is shown. Notice the structure in the distribution of sample points which makes the sampling density highly non-isotropic, except in the mid-frequency range. (b) With the same number of beams, spacing between adjacent beams are sinusoidally modulated. Resulting sample points are more randomly distributed, reducing non-isotropy in density.

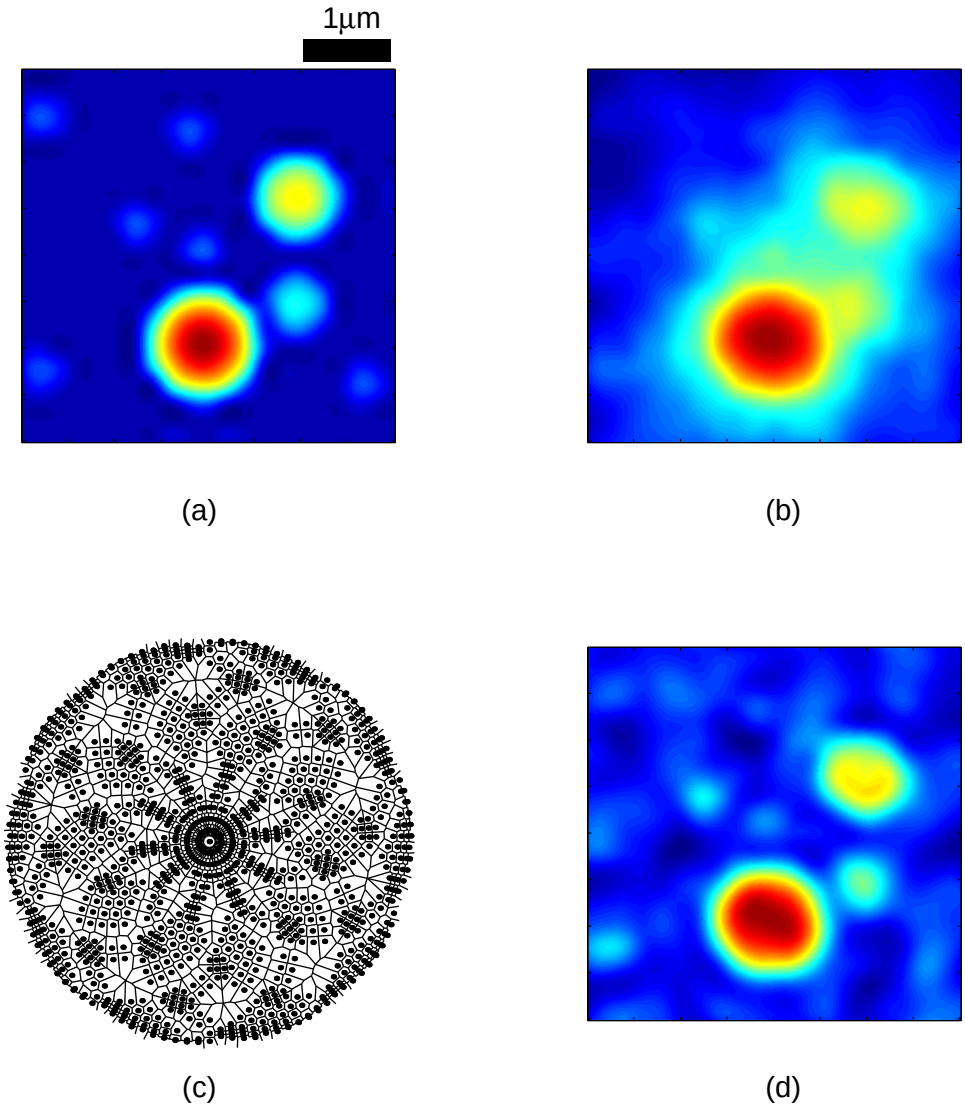

Figure 7: Simulated image reconstruction for 35 beam SAM in figure 5. (a) Synthetic image of a hypothetical sample. Constellation of microbeads with various sizes are shown. Smaller beads are less bright than bigger ones. (b) Reconstruction without weighting Fourier coefficients. Due to non-isotropy in sampling density shown in figure 5, smearing effect of bigger beads obscures smaller, less bright ones. (c) Calculation of weights for Fourier sample points. For each sample point, area of Voronoi polygon surrounding it is computed and assigned as a weight. (d) Reconstruction with weighting Fourier coefficients. Weighting effectively treats artifacts found in panel (b), thereby improving resolution.

microscopy. Through this exploration, SAM will be shown to be a viable tool in biology and medicine.

Figure 8: Two possible applications of SAM. (a) *in vitro* culture of neurons (from [**5**]). Synapses are fluorescently labeled and show up as red. The image was acquired with confocal laser scanning microscope with 1 μm resolution. (b) DNA microarray. Each spot, circular in shape, is about 200 μm in diameter and contains fluorescently labeled nucleotides representing different genes.

References

[1] D. A. Agard and J. W. Sedat. Three-dimensional architecture of polytene nucleus. *Nature*, 302:676–681, 1983.

[2] W. A. Carrington, R. M. Lynch, E. D. W. Moore, G. Isenberg, K. E. Fogarty, and F. S. Fay. Superresolution three-dimensional images of fluorescence in cells with minimum light exposure. *Science*, 268:1483–1487, 1995.

[3] W. J. Denk, D. W. Piston, and W. W. Webb. Two-photon molecular excitation laser scanning microscopy. In J. B. Pawley, editor, *Handbook of Biological Confocal Microscopy*, pages 445–58. Plenum, New York, 1995.

[4] W. J. Denk, J. H. Strickler, and W. W. Webb. Two-photon laser scanning fluorescence microscopy. *Science*, 248:73–76, 1990.

[5] G. P. Fan, C. Egles, Y. Sun, J. Minichiello, J. J. Renger, R. Klein, G. Liu, and R. Jaenisch. Knocking nt4 into the bdnf gene locus not only rescues bdnf deficient mice but also reveals their distinct activities *in vivo*. *Nature Neurosci.*, 3:350–357, 2000.

[6] J. T. Frohn, H. F. Knapp, and A. Stemmer. True optical resolution beyond the Rayleigh limit achieved by standing wave illumination. *Proc Natl Acad Sci USA*, 97:7232–7236, 2000.

[7] S. W. Hell and E. H. K. Stelzer. Properties of a 4pi-confocal fluorescence microscope. *J. Opt. Soc. Am. A*, 9:2159–2166, 1992.

[8] T. J. Holmes. Maximum-likelihood image restoration adapted for noncoherent optical imaging. *J. Opt. Soc. Am. A*, 5:666–673, 1988.

[9] R. A. Hutchin. Microscope for producing high resolution images without precision optics. U.S. Patent No. 4,584,484, 1986.

[10] F. Liu, S. Nie, C. Tao, and S. Bian. Theory and computer simulation of the synthetic aperture microscopy. *Proceedings of the SPIE*, 2890:58–62, 1996.

[11] M. S. Mermelstein. *Synthetic aperture microscopy.* PhD thesis, Massachusetts Institute of Technology, Cambridge, MA, 2000.

[12] J. Ryu, M. S. Mermelstein, and D. M. Freeman. Phase calibration for synthetic aperture microscopy. In *Poster presentation*, Cambridge, MA, March 2000. the 13th annual Health Sciences and Technology forum.

[13] T. Turpin. Image synthesis using time sequential holography. U.S. Patent No. 5,751,243, 1998.

[14] T. Turpin, L. Gesell, J. Lapides, and C. Price. Theory of the synthetic aperture microscopy. *Proceedings of the SPIE*, 2566:230–240, July 1995.

[15] T. Wilson. Optical sectioning in confocal fluorescent microscopes. *J. Microsc.*, 154:143–156, 1989.